Middle ear cholesteatoma extending into the petrous apex: evaluation by CT and MR imaging.

K Ishii, S Takahashi, K Matsumoto, T Kobayashi, T Ishibashi, K Sakamoto and T Soda

AJNR Am J Neuroradiol 1991, 12 (4) 719-724
http://www.ajnr.org/content/12/4/719

Middle Ear Cholesteatoma Extending into the Petrous Apex: Evaluation by CT and MR Imaging

Kiyoshi Ishii[1]
Shoki Takahashi[1]
Ko Matsumoto[1]
Toshimitsu Kobayashi[2]
Tadashi Ishibashi[1]
Kiyohiko Sakamoto[1]
Toyoji Soda[3]

CT and MR imaging findings were reviewed in four cases of acquired cholesteatoma of the middle ear that extended medially into the petrous apex and middle cranial fossa. In one case the lesion further extended anteromedially into the sphenoid sinus. CT demonstrated the lesions as nonenhancing hypodense masses with bone destruction, extending medially from the middle ear cavity to the petrous apex region. On MR imaging, the lesion was slightly hypointense relative to brain on T1-weighted images and hyperintense on T2-weighted images. MR imaging clearly delineated the extraaxial location of the lesion and associated brain displacement. The medial extension of the cholesteatomas seems to have proceeded via a detour around the bony labyrinth into the petrous apex region by following normal pathways of temporal bone pneumatization.

AJNR 12:719–724, July/August 1991

Cholesteatomas of the temporal bone are usually acquired lesions that occur in the middle ear cavity. They are thought to be caused by ingrowth of keratinizing squamous epithelium from the external ear. As they enlarge and come in contact with the contiguous bony structures of the middle ear, erosion of the bony structures occurs as a result of pressure necrosis and enzymatic lysis of the bone [1–3]. Although there are many complications associated with cholesteatomas of the middle ear [1–4], extension into the petrous apex is extremely rare [1, 3–9]. We describe the CT and MR findings in four patients with an acquired cholesteatoma of the middle ear that extended medially into the petrous apex. In one case the lesion further extended into the clivus and the sphenoid sinus.

Materials and Methods

Four patients with cholesteatoma of the middle ear that extended into the petrous apex region were studied. All four patients had surgery, and cholesteatoma was verified histologically. CT scans were obtained in all four cases by using a high-resolution algorithm for temporal bone evaluation. MR images were obtained in two of the four cases, and these studies were performed on a 1.5-T system. For each of these patients, both axial, spin-echo, T1-weighted 500/15/4 (TR/TE/excitations) and T2-weighted, 2500/90/1, images were obtained using a surface coil of 6-cm diameter.

Results

Clinical and neurootologic findings in the four cases are summarized in Table 1. All the patients had a history of chronic otitis media of long duration together with conductive and/or sensorineural hearing loss. Three patients also had facial palsy, while the fourth patient exhibited lower cranial nerve palsies. Two of the four patients (cases 1 and 4) had had prior middle ear surgery for cholesteatoma.

High-resolution CT of the temporal bone showed a soft-tissue lesion in the petrous apex region. In each case, the mass in the petrous apex region appeared

Received August 16, 1990; revision requested December 21, 1990; revision received January 25, 1991; accepted February 7, 1991.

[1] Department of Radiology, School of Medicine, Tohoku University, Seiryo-machi 1-1, Aoba-Ku, Sendai 980, Japan. Address reprint requests to K. Ishii.

[2] Department of Otolaryngology, School of Medicine, Tohoku University, Sendai 980, Japan.

[3] Department of Otolaryngology, School of Medicine, Fukuoka University, Fukuoka 814-01, Japan.

0195-6108/91/1204-0719

to be continuous laterally with an opacity in the middle ear cavity (Figs. 1–4). The density of the lesions was slightly lower than that of brain and slightly higher than that of CSF. Most of the bony labyrinth was well preserved although small, focal areas of erosion were seen in three patients (cases 1, 3, and 4). In the fourth patient (case 2), the otic capsule was diffusely thinned, although the bony remnants of the capsule still outlined the majority of the labyrinthine structures, indicating that most of these structures were in large part preserved. There was no contrast enhancement in or around the lesion after IV infusion of contrast material. In case 1, the lesion extended further anteromedially into the clivus and the sphenoid sinus, displacing the pituitary gland upward and the ipsilateral cavernous sinus anteriorly.

MR images in the two cases studied showed the lesions to be slightly hypointense relative to adjacent brain on T1-weighted images and hyperintense on T2-weighted images. Curvilinear hypointense signals were observed over the surface of the lesion, which helped to define the contour of the lesions. The curvilinear hypointensity was thought to represent the remaining bony structures and/or the dura displaced around the lesion. Preserved bony labyrinths were revealed in each case as an area of signal loss, partially encompassed by the lesions.

Judging from the appearance of the lesions on CT and MR images, the connection between the petrous apex lesions and the middle ear cavity was located anteroinferior to the cochlea in case 1, anteroinferior and anterosuperior to the cochlea in case 2, anterosuperior and posterosuperior to the bony labyrinth in case 3, and anterosuperior to the cochlea in case 4.

Surgery was performed in all four cases and a cholesteatoma involving the petrous apex region and middle ear cavity was verified in each case. The sphenoid sinus involvement in case 1 was also surgically verified.

TABLE 1: Clinical Findings in Four Patients with Acquired Cholesteatoma

Case No.	Age	Sex	Duration of COM (years)	Symptoms
1	28	F	22+	CHL, SNHL, facial palsy, nausea, vomiting
2	33	M	12	CHL, SNHL, headache, IX–XI cranial nerve palsy
3	49	M	20	CHL, facial palsy
4	54	F	45	CHL, SNHL, facial palsy

Note.—COM = chronic otitis media, CHL = conductive hearing loss, SNHL = sensorineural hearing loss.

Discussion

Cholesteatomas of the middle ear are thought to be the result of ingrowth of keratinizing squamous epithelium from the external ear. Erosion occurs as they enlarge and come in contact with contiguous bony structures of the middle ear [1–3]. There are many complications of cholesteatomas of the middle ear, including ossicular destruction, automastoidectomy, labyrinthine fistula, facial nerve palsy, meningitis, dural sinus thrombosis, and petrous apex extension [1–4]. Although extension of cholesteatomas outside the middle ear cavity is a well-known entity, such a mode of extension occurs infrequently, and very few reports have described the CT and/or MR imaging findings [3–6, 8].

In cases of medial extension of cholesteatoma, extension tends to occur through sites of least resistance, thus taking one or more of the following three paths [1] (see Fig. 5): (1) the infralabyrinthine route, inferior to the cochlea and internal auditory canal, potentially breaching into the jugular fossa; (2) the anterosuperior route above the cochlea, involving the geniculate ganglion and suprameatal area of the petrous bone; and (3) the posterosuperior route, between the limbs of the superior semicircular canal to reach the fundus of the internal auditory canal, potentially broaching a wall of the internal auditory canal.

In the four cases in the present study, the cholesteatoma in case 1 probably extended via the infralabyrinthine route, that in case 2 via both the anterosuperior and the infralabyrinthine routes, that in case 3 via both the antero- and posterosuperior routes, and that in case 4 via the anterosuperior route. The cochlea appeared to be intact in three patients (cases 1, 3, and 4), while thinned remnants outlined the labyrinth in the remaining patient (case 2). As the bony laby-

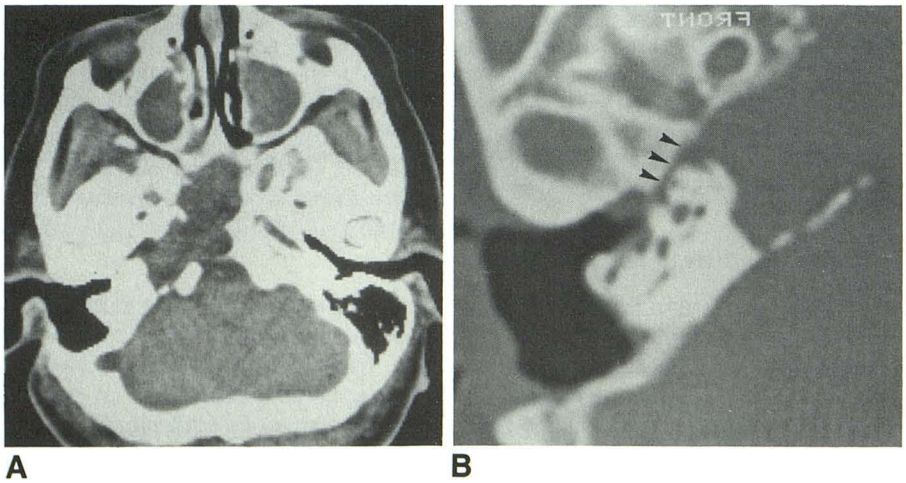

Fig. 1.—Case 1.

***A*, Plain axial CT scan reveals a soft-tissue lesion that is slightly hypodense relative to brain involving the petrous apex, clivus, and sphenoid sinus with extensive bone destruction. There is no contrast enhancement in the lesion (not shown).**

***B*, High-resolution axial CT scan right temporal bone shows soft-tissue lesion in petrous apex to be continuous with the middle ear cavity through an isthmus of bone erosion through the cupula cochleae (*arrowheads*). Most of the labyrinthine system is preserved.**

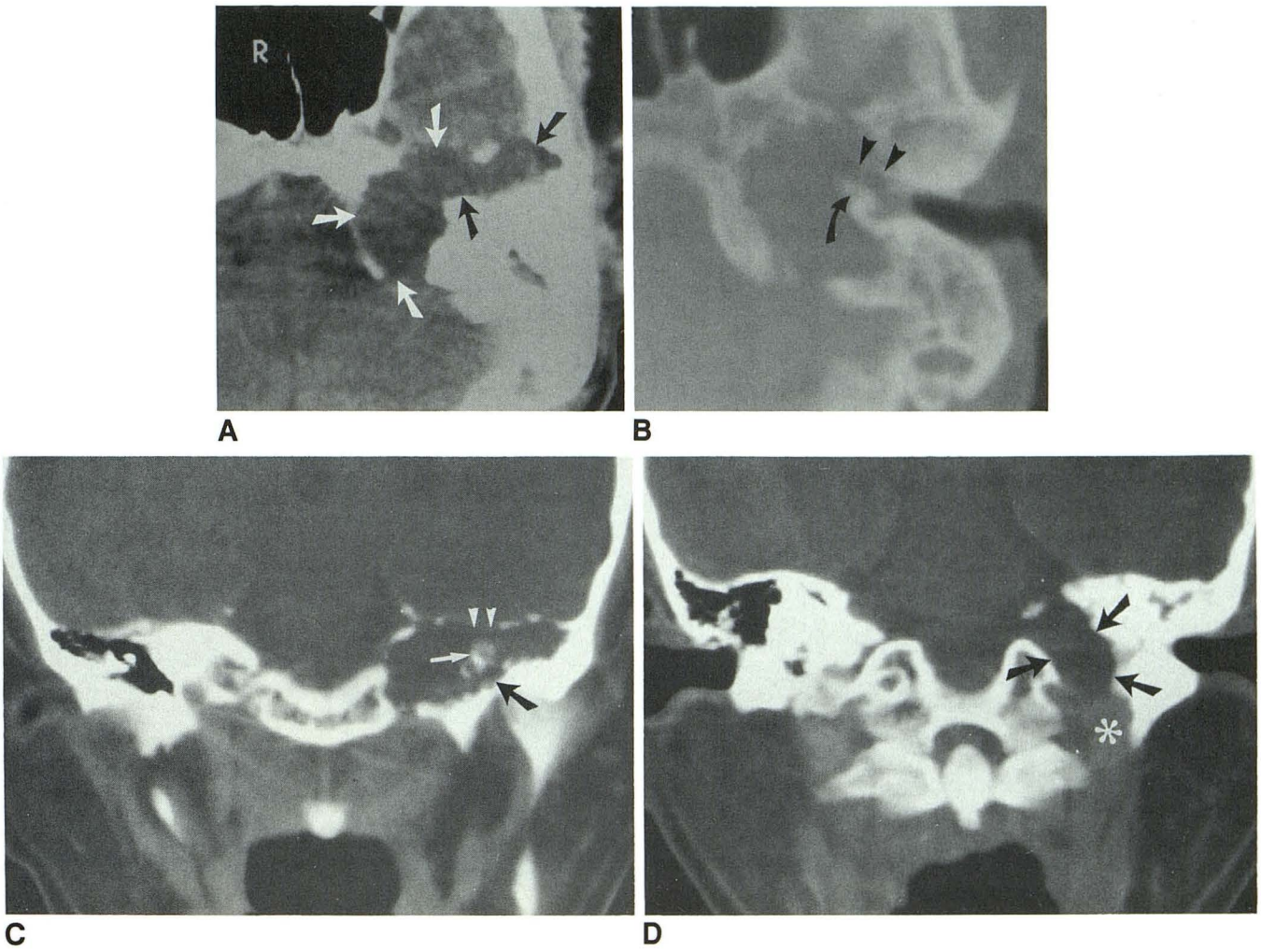

Fig. 2.—Case 2.

***A*, Plain axial CT scan of left temporal bone discloses a slightly hypodense mass involving the petrous apex with scalloped bone destruction (*arrows*).**

***B*, CT scan with bone window settings shows that the petrous apex lesion is continuous with left middle ear cavity (*arrowheads*). A residual part of the cochlea is identified (*curved arrow*).**

***C*, Coronal CT scan discloses a soft-tissue lesion involving the left petrous apex region, which can be followed laterally into the middle ear cavity, passing both superiorly (*white arrowheads*) and inferiorly (*black arrow*) to thinned remnant of cochlea (*white arrow*).**

***D*, Enhanced coronal CT scan just posterior to *C* shows lesion extending to enlarged left jugular foramen (*arrows*). The internal jugular vein is identified by contrast enhancement (*asterisk*).**

rinth is one of the densest bones in the body, it is more resistant to erosion. According to Valvassori and Buckingham [1], petrous extension of acquired cholesteatomas occurs in large cholesteatomas that arise in a well-pneumatized petrous bone. The paths of extension of the acquired cholesteatomas mentioned above were also well correlated with the distribution of temporal bone pneumatization evaluated by Virapongse et al. [10]. Therefore, medial extension of cholesteatomas usually takes a detour around the bony labyrinth as it extends to the petrous apex.

Differential diagnoses of a petrous apex mass lesion include neurinoma (especially of the fifth cranial nerve), chordoma, bony or cartilaginous tumor, paraganglioma, metastasis, cholesterol granuloma, giant cholesterol cyst, infected mucocele, congenital epidermoid, and extension of middle ear cholesteatoma [1, 11–14]. In the case of neoplastic lesions, excluding congenital epidermoid tumor, contrast enhancement can be seen on both CT and MR studies. On CT images, cholesterol granuloma, giant cholesterol cyst, mucocele, and congenital epidermoid tend to look similar to one another as well as to medial extension of a middle ear cholesteatoma [12–14] with respect to density and absence of contrast enhancement. Infected mucocele (pyocele) may sometimes show a thin rim of contrast enhancement; however, findings are almost the same as those for mucocele. The most common treatment of choice for cholesterol granuloma, giant cholesterol cyst, and mucocele is simple drainage with or without permanent fistulization, while the treatment for either an extensive middle ear cholesteatoma or congenital epidermoid in the petrous apex essentially requires surgical excision. Given the different types of treatment for these two groups of lesions, preoperative differential diagnosis is important.

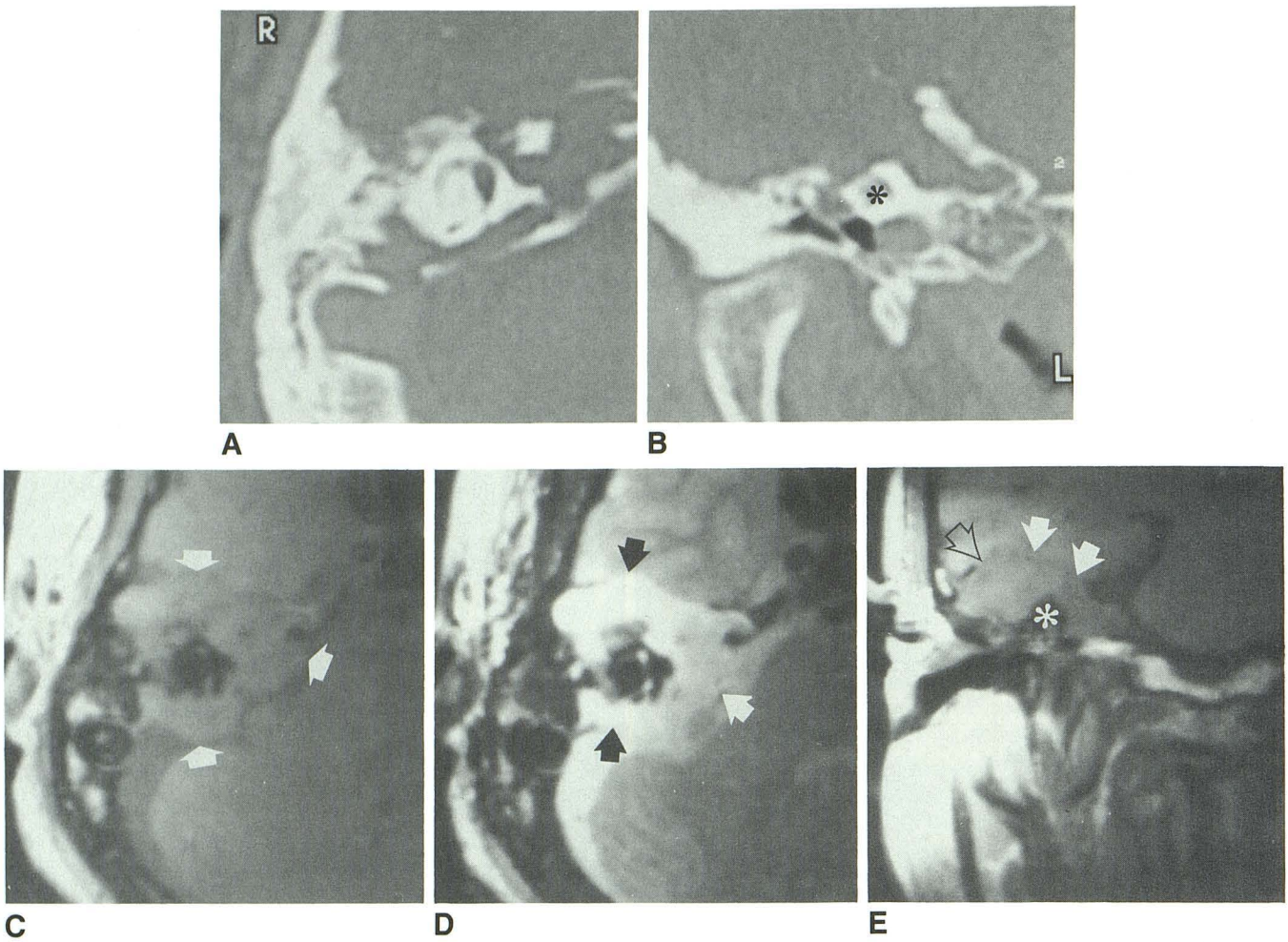

Fig. 3.—Case 3.

A, Axial CT scan of right temporal bone reveals a soft-tissue mass involving the right petrous apex region with extensive bone destruction. The lesion can be followed laterally to the attic and mastoid regions around the bony labyrinth.

B, Coronal CT scan shows lesion to be continuous with a middle ear opacity over the cochlea (*asterisk*).

C, T1-weighted MR image (500/15) of right temporal bone reveals a mass of intermediate signal intensity in right pyramid (*white arrows*). Curvilinear hypointense signal is seen over the surface of the mass lesion, which helps identify the contour of the lesion. Preserved bony labyrinth is seen as a structure of signal void in the center.

D, T2-weighted MR image (2500/90) shows mass as hyperintense lesion (*arrows*) that bulges anteriorly into middle cranial fossa and posteriorly into cerebellopontine angle region.

E, Coronal T1-weighted image shows that mass extends superiorly to the bony labyrinth (*asterisk*) and elevates the temporal lobe (*arrows*). Curvilinear hypointense signal is also seen over the surface of the mass lesion, which may represent the remaining bony structures and/or the dura displaced around the lesion.

Cholesteatoma usually appears to be a well-defined, homogeneous, and hypodense mass on noncontrast CT scans. The margins of the bone adjacent to the bony labyrinth may be sclerotic and scalloped [13]. On MR images, a cholesteatoma appears as a lesion of low or intermediate signal intensity on T1-weighted sequences and one of high signal intensity on T2-weighted sequences [15, 16]. This conforms exactly to the findings in the two cases reported here.

Cholesterol granuloma, caused by chronic obstruction of normally pneumatized spaces in the temporal bone, is covered by a fibrous capsule and is filled with brownish or yellowish liquid containing cholesterol crystals, hemorrhagic products, and/or proteinaceous debris. On CT the lesion appears as an ovoid homogeneous mass that is isodense with brain. There is bone erosion without calcification and no contrast enhancement except for the overlying dura [13, 14]. On MR imaging, the lesion appears hyperintense on both T1- and T2-weighted sequences with a peripheral hypointense margin on T2-weighted sequences [17]. MR imaging seems to delineate more specific features of cholesterol granuloma than does CT, thus permitting correct diagnosis of this lesion.

Giant cholesterol cyst is filled with glistening brown, watery fluid containing cholesterol crystals and lined by a fibrous capsule. On CT, the lesion appears to be isodense with brain, with a peripheral rim of contrast enhancement [12]. MR imaging findings have not yet been reported.

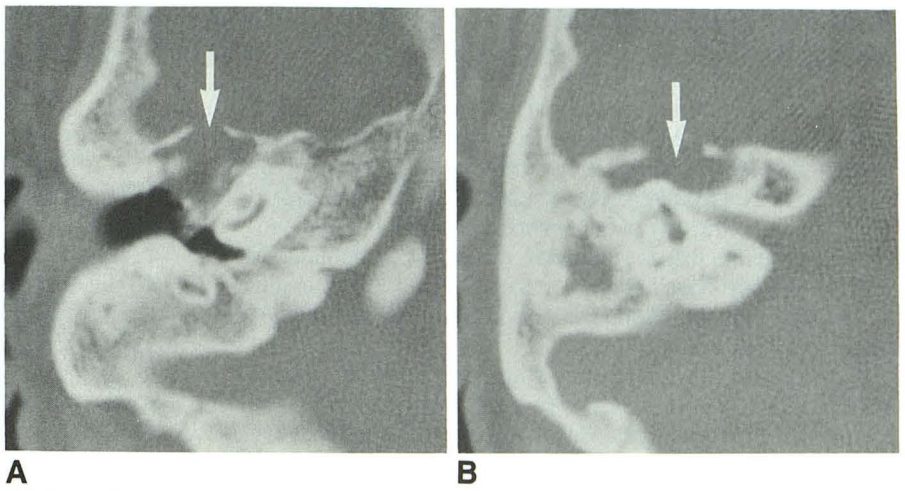

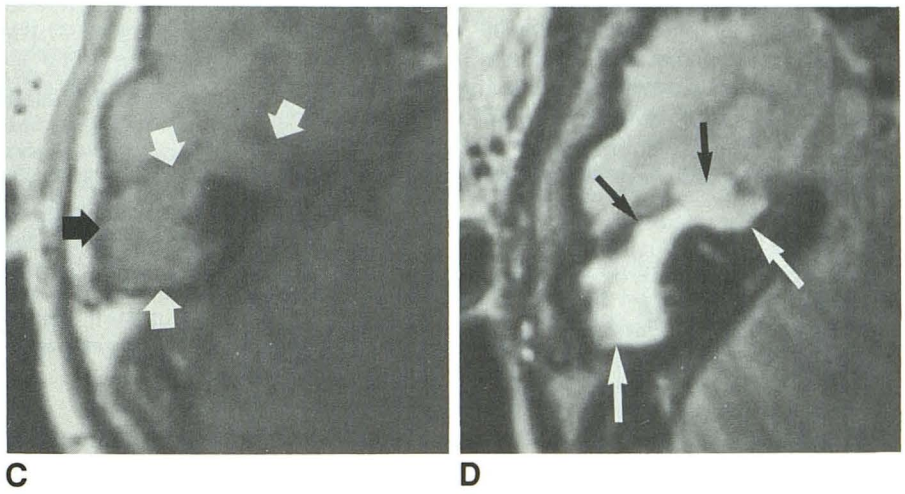

Fig. 4.—Case 4.

A, Axial CT scan of temporal bone reveals a soft-tissue mass in anterior aspect of middle ear cavity that projects anteriorly into middle cranial fossa through an area of bone destruction (*arrow*).

B, Axial CT scan at higher level than *A* shows the lesion extending anteromedially into petrous appex (*arrow*). Bony labyrinth is well preserved.

C, Axial T1-weighted MR image (500/15) discloses a well-demarcated intermediate signal intensity mass (*arrows*). Curvilinear hypointense signal is also seen over surface of mass. Bony labyrinth appears as area of signal loss in posterior aspect of mass.

D, Axial T2-weighted MR image (2500/90) shows mass to be hyperintense (*arrows*). Otic capsule is revealed as an area of signal void.

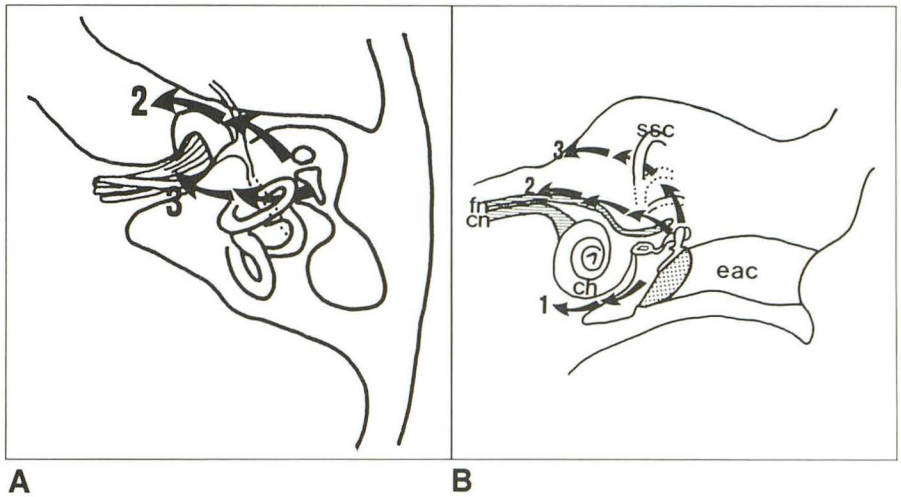

Fig. 5.—*A* and *B*, Schematic representations of routes of extension of cholesteatoma; horizontal (*A*) and coronal (*B*) schemes. *Arrows* indicate the routes of extension of middle ear cholesteatoma.

1 = infralabyrinthine route, inferior to cochlea and internal auditory canal, 2 = anterosuperior route above the cochlea, involving the geniculate ganglion and suprameatal area of petrous bone, 3 = posterosuperior route between the limbs of the superior semicircular canal to reach the fundus of the internal auditory canal. fn = facial nerve, cn = cochlear nerve, ch = cochlea, ssc = superior semicircular canal, eac = external auditory canal.

Modified from Silver et al. [3].

Mucocele usually appears to be isodense with CSF and sometimes shows marginal enhancement, which on CT may represent the overlying dura [13]. MR imaging shows the lesion as hyperintense on T2-weighted sequences but as variably intense on T1-weighted sequences, depending on the proteinaceous density in its content. Infected mucocele shows nearly similar findings to mucocele.

Taking the characteristic features mentioned above into consideration, it is possible to differentiate cholesteatomas from cholesterol granuloma, giant cholesterol cyst, and mu-

cocele, especially by density on CT and signal intensity on MR imaging.

The petrous apex is also the preferential site of congenital epidermoid, which would show similar density on CT and similar intensity on MR imaging to an extensive middle ear cholesteatoma. Congenital epidermoid of the petrous apex, however, is extremely rare, and patients with this lesion would not have a prior history of otitis media. Furthermore, congenital epidermoid in the petrous apex would not be continuous with middle ear opacification on both CT and MR imaging, which would clearly distinguish it from an extensive cholesteatoma of the middle ear.

In conclusion, CT and MR imaging findings in four cases of cholesteatoma with petrous apex extension were reviewed. CT demonstrated the lesion as a nonenhancing hypodense mass in the petrous apex region with bone destruction, which appeared to be continuous laterally with an opacity in the middle ear cavity. MR imaging revealed the mass as hypointense on T1-weighted sequences and hyperintense on T2-weighted sequences. The medial extension of the cholesteatomas in these cases seems to have proceeded via a detour around the bony labyrinth into the petrous apex region by following normal pathways of temporal bone pneumatization.

REFERENCES

1. Valvassori GE, Buckingham RA. Radiology of the temporal bone. In: Valvassori GE, Buckingham RA, Carter BL, et al. eds. *Head and neck imaging*. Stuttgart: Thieme, **1988:**1–172
2. Swartz JD. Cholesteatomas of the middle ear: diagnosis, etiology, and complications. *Radiol Clin North Am* **1984**;22:15–35
3. Silver AJ, Janecka I, Wazen J, et al. Complicated cholesteatomas: CT findings in inner ear complications of middle ear cholesteatomas. *Radiology* **1987**;164:47–51
4. Johnson DW, Hinshaw DB Jr, Hasso AN, et al. Computed tomography of local complications of temporal bone cholesteatomas. *J Comput Assist Tomog* **1985**;9:519–523
5. Sheehy JL. Residual cholesteatoma in the middle cranial fossa: a case report. *Am J Otol* **1984**;5:227–228
6. Kreutzer EW, DeBlane GB. Extra-aural spread of acquired cholesteatoma. *Arch Otolaryngol* **1982**;108:320–323
7. Arkin CF, Millard M, Medeiros J. Giant invasive cholesteatoma. Report of a case of cerebellar invasion. *Arch Pathol Lab Med* **1985**;109:960–961
8. Sultan AA. Cholesteatomas of the temporal bone invading the posterior and middle cranial fossa. *Adv Otorhinolaryngol* **1987**;37:138–140
9. Yanagihara N, Matsumoto Y. Cholesteatoma in the petrous apex. *Laryngoscope* **1981**;91:272–278
10. Virapongse C, Sarwar M, Bhimani S, Sasaki C, Shapiro R. Computed tomography of temporal bone pneumatization: 1. Normal pattern and morphology. *AJNR* **1985**;551–559
11. Flood LM, Kemink JL. Surgery in lesions of the petrous apex. *Otolaryngol Clin North Am* **1984**;17:565–575
12. Latak JT, Graham MD, Kemink JL, Knake JE. Giant cholesterol cysts of the petrous apex: radiologic features. *AJNR* **1985**;8:409–413
13. Lo WWM, Solti-Bohman LG, Brackmann DE, et al. Cholesterol granuloma of the petrous apex: CT diagnosis. *Radiology* **1984**;153:705–711
14. Greenberg JJ, Oot RF, Wismer GL, et al. Cholesterol granuloma of the petrous apex: MR and CT evaluation. *AJNR* **1988**;9:1205–1214
15. Latak JT, Kartush JM, Kemink JL, et al. Epidermoidomas of the cerebellopontine angle and temporal bone: CT and MR aspects. *Radiology* **1985**;157:361–366
16. Tampieri D, Melanson D, Ethier R. MR imaging of epidermoid cysts. *AJNR* **1989**;10:351–356
17. Martin N, Sterkers O, Mompoint D, et al. Cholesterol granuloma in the middle ear cavities: MR imaging. *Radiology* **1989**;172:521–525